An Application of Time Series Analysis for Forecasting and Control of Carbon Monoxide Concentrations

Claudio Guarnaccia, Julia Griselda Cerón Bretón, Joseph Quartieri, Carmine Tepedino and Rosa Maria Cerón Bretón

***Abstract*—**In large urban areas, where many activities occur due to a big number of citizens, physical polluting agents should be carefully assessed in order to protect human health. The monitoring and control of air pollution, acoustical noise, electromagnetic fields, etc., represent a relevant problem to be considered. Therefore, the development of mathematical models able to predict the air pollution behaviour is a very important field of research. In this paper, the authors will use a model based on Time Series (TS) analysis. A large set of field measurements is reconstructed by an appropriate functional form. The proposed model can evaluate the trend and the periodic pattern in the calibration dataset, and can forecast the slope in any future time range. The TS analysed in this work is composed by hourly CO concentrations observed in the urban site of San Nicolas de los Garza, Nuevo Leon, Mexico. To calibrate the model's parameters, a large set of one year field measurements will be analysed: this procedure will highlight a periodicity of 24 hours in the dataset and a substantial absence of any relevant trend. The authors will perform also a validation of the model on two different months, using data not adopted in the calibration phase. This procedure will show that the model is able to reproduce the overall trend and the periodic behaviour present in the large part of the dataset but, at the same time, it cannot predict isolated peaks or sudden fall of CO concentration. In addition, a Principal Component Analysis will be applied to a data set for one year period in order to investigate the relation among CO concentrations and other measured parameters (meteorological conditions and air criteria pollutants). Resulting principal components can be used in future multiple regression analysis in order to mitigate multicollinearity.

***Keywords*—**Air Pollution, Criteria Pollutants, CO Concentration, Principal Component Analysis, Regression Analysis, Time Series.

I. Introduction

THE physical and chemical processes of atmospheric pollutants gases, particularly nitrogen oxides (NO_x), CO and volatile organic compounds (VOC), in the low atmosphere result in the formation of secondary oxidized products. Since many of these processes are regulated by the presence of sunlight, the oxidized products are commonly referred to as "secondary photochemical pollutants" being Ozone (O_3), the most important oxidant at the troposphere [1].

Tropospheric ozone has been recognized as one of the most important atmospheric oxidants in urban areas ([2], [3]), the primary source of OH radicals and the third most important greenhouse gas behind CO_2 and CH_4. In the stratosphere, ozone helps to block an excessive ultraviolet irradiation of the earth but at the troposphere, this pollutant has been related to adverse effects on human health, vegetation and materials ([4-11]).

In urban areas, CO is one of the most important ozone precursors as it is known to be a tracer of vehicle exhaust emissions. Its outdoor sources include diverse anthropogenic activities such as power station burning coal, combustion of fossil fuels, making steel, etc.. Indoor sources of this pollutant include tobacco smoke and biomass burning from cooking and houses warming systems. In addition, CO it is known to be toxic and cause several health affections. CO poisoning is the most common type of fatal poisoning in many countries. Symptoms of mild poisoning include headaches, vertigo, and flu-like effects. Larger exposures can lead to significant toxicity of the central nervous system, heart and even death. Following poisoning, long-term sequelae often occurs. Carbon monoxide can also have severe effects on the fetus of a pregnant woman [12]. In developed countries, as for instance United States, it has been estimated that more than 40000 people per year seek medical attention for carbon monoxide poisoning [13].

For all these reasons it is important to know the behaviour and trends of CO in a given site and to understand the role that this pollutant plays in the tropospheric ozone formation. The main atmospheric sink process for CO is by reaction with OH, and this mechanism also makes CO a major precursor to photo chemical ozone [14].

The day time increase in ozone concentration, which is a pronounced feature of a polluted site, it is basically due to the photo-oxidation of the precursor gases such as CO, CH_4 and NMHC (non methane hydrocarbons) in the presence of sufficient amount of NO_x. In this process NO_x acts as a catalyst and continues to do so until physical processes permanently remove it or it gets transformed to other oxides of nitrogen. The well-known photo-oxidation cycle of CO can be

C Guarnaccia, J. Quartieri, C. Tepedino are with the Department of Industrial Engineering, University of Salerno, Via Giovanni Paolo II, I-84084 Fisciano (SA) – ITALY (corresponding author: cguarnaccia@unisa.it , quartieri@unisa.it , ctepedino@unisa.it).

J. G. Cerón Bretón and R. M. Cerón Bretón are with the Environmental Sciences Research Center, Autonomous University of Carmen City (UNACAR), Av. Abasolo s/n Col. Renovación 2da Sección, CP 24180, Ciudad del Carmen, Campeche – MEXICO (jceron@pampano.unacar.mx , rceron@pampano.unacar.mx).

represented as [15]:

$$CO + OH \rightarrow CO_2$$
$$H + O_2 + M \rightarrow HO_2 + M$$
$$HO_2 + NO \rightarrow NO_2 + OH$$
$$NO_2 + hv \rightarrow O(^3P) + NO$$

$$\lambda < 420 \text{ nm}$$

$$O(^3P) + O_2 + M \rightarrow O_3 + M$$

Net: $CO + 2O_2 + hv \rightarrow CO_2 + O_3$

Therefore, accurate characterization of CO is extremely important for understanding tropospheric ozone formation and accumulation, and crafting effective control strategies to better address ozone air quality management issues. However, the continuous monitoring of air pollutants is generally expensive; most of the times it is limited only to big urban areas and usually the number of the stations of the air quality monitoring networks are not enough. Therefore, there is growing need to implement predictive models that can provide a reliable assessment in an economical way of air pollution levels and other polluting agents (see for instance [16-25]). Among these models, Time Series Analysis (TSA) models ([26], [27]) have been largely adopted in several disciplines and have showed good performances and adaptability to polluting agents levels prediction ([28-31]).

This paper aims to apply TSA models to the hourly CO concentrations dataset collected in an urban site of San Nicolas de los Garza, Nuevo Leon, Mexico. Once the model is calibrated on a given dataset, a validation on more than one range of observed values (not used in the calibration) will be performed, in order to estimate the predictive performances and to understand the criticalities of the model. In addition the relation among CO and other parameters (meteorological conditions and air criteria pollutants) is investigated by a Principal Component Analysis (PCA) in order to obtain the a group of parameters that could influence the CO levels in the studied site.

II. Methods

The model adopted in this paper has been presented by some of the authors in [28]. It is based on the Time Series analysis (TSA) models idea. These TSA are mathematical models largely adopted in Economics, Physics, Engineering, Mathematics, etc.. (see for instance [32-34]), that are used to reproduce the behaviour of data series and to predict future slope.

The main aims of these kind of models are basically the recognition of the phenomenon under study by means of data trend and periodicity reconstruction, and the prediction of future values of the time series. Thus, a general procedure may be resumed as follows:

- Possible seasonal effect detection in the data set
- Lag (periodicity) evaluation
- Smoothing (removal of periodicity) of the calibration data time series
- Trend and seasonality evaluation
- Error evaluation (difference between observed and forecasted values in the calibration dataset)
- Final model drawing

The details of how perform the steps listed above can be found in [28] and references therein, where different approaches, in particular additive and multiplicative, are presented and briefly discussed. The choice for this dataset is a mixed approach, that is multiplicative between trend and seasonality, and additive for the error component:

$$F_t = T_t \bar{S}_i + m_e \quad (1)$$

where F_t is the model prediction, T_t is the trend, $\bar{S}_i$ is the seasonal coefficient, m_e is the mean of the error e_t, defined as actual value (A_t) minus forecast (F_t):

$$e_t = A_t - F_t \quad (2)$$

Let us underline that TSA models are mostly adopted when the data sets follow recurring seasonal patterns. The attempt to adopt this kind of models in a so variable and random physical phenomenon, such as air pollution, is extremely challenging. Results shown in Section IV will underline these difficulties and open new ways to further improvement of this model.

A. Detection of the presence of a lag

The presence of a periodicity in the series can be detected adopting the Ljung-Box (LB) or the Box-Pierce (BP) tests ([35], [36]). These tests verify if the data have an autocorrelation and they may exclude the presence of fully random data fluctuations. Both tests adopt the autocorrelation coefficient that may be evaluated according to the following formula:

$$r(k) = \frac{\sum_{t=1}^{n-k}(x_t - \bar{x})(x_{t+k} - \bar{x})}{\sum_{t=1}^{n}(x_t - \bar{x})^2} , \quad (3)$$

where x_t is the data in each period t, $\bar{x}$ is the mean of all the data, n is the total number of periods, k is the lag hypothesis under test. Using this coefficient, the LB test can be performed according to the following formula:

$$\chi^2_{LB}(h) = n(n+2)\sum_{k=1}^{h}\frac{r^2(k)}{n-k} , \quad (4)$$

where h is a chosen integer related to the number of autocorrelation coefficients under test, and it varies according to the assumed lag.

If the null hypothesis is true (absence of autocorrelation), the LB statistics is distributed according to a random variable χ^2, with h degree of freedom.

The BP test is based on the following formula:

$$\chi^2_{BP}(h) = n\sum_{k=1}^{h} r^2(k) \quad , \tag{5}$$

where, again, *n* is the total number of periods, *k* is the assumed lag and *h* is a chosen integer, related to the number of autocorrelation coefficients under test. The two tests differ only in the different weighting systems adopted, but asymptotically converge to the same distribution.

B. Error metrics

As in [28] and [29], a measurement of model performance can be obtained by "mean percentage error" (MPE) and "coefficient of variation of the error" (CVE). The first quantitative metric gives a measurement of the error distortion, i.e. MPE is able to describe if the model overestimates or underestimates the actual data. CVE considers the variation from the reality in absolute value. In other words, it provides the error dispersion. Those metrics are evaluated according to the following formulas:

$$MPE = \frac{\sum_{t=1}^{n}\left(\frac{A_t - F_t}{A_t}\right)100}{n} \tag{6}$$

and

$$CVE = \frac{\sqrt{\frac{\sum_{t=1}^{n}(e_t)^2}{n-1}}}{\bar{A}} \quad , \tag{7}$$

where $\bar{A}$ is the mean value of the actual data in the considered time range.

C. Error distribution analysis tools

It is necessary to verify that the mean of the errors (residuals) is not different from zero, in statistical sense. In this paper the authors use the *t*-test:

$$t = \frac{\bar{e}}{s/\sqrt{n}} \quad , \tag{8}$$

where $\bar{e}$ is the mean of the error, *s* is the standard deviation and *n* is the amount of data.

The null hypothesis H_0 is "mean equal to zero". Thus in the numerator of equation (8) there is only the empirical mean (since usually the empirical mean minus the hypothesized one is adopted). In this type of test it is possible to have two type of errors. The first is to reject H_0 when it is true (it can happen with probability α, i.e. the significance level). The second one is to accept H_0 when it is false (this can happen with probability β, and $1 - \beta$ is the power of the test).

It is important to check if the random errors obtained by the model application can be drawn from a normal distribution. To assess the normality of the distribution of errors, the authors proposed both qualitative techniques based on the analysis of graphs such as histogram, QQ normality plot and quantitative indices, namely skewness and kurtosis. In particular, the normal density plot [37] is a graphical technique for assessing whether or not a data set is approximately normally distributed. The data are plotted against a theoretical normal distribution in such a way that the points should form an approximate straight line. Deviations from this straight line indicate deviations from normality.

D. Principal Component Analysis

The relation among CO concentrations and other parameters (meteorological conditions: solar radiation, wind speed, wind direction, temperature, barometric pressure and relative humidity; and other air criteria pollutants: O_3, NO, NO_2, NO_x, PM_{10}, $PM_{2.5}$ and SO_2) can be investigated by a factor analysis in order to obtain a pattern recognition study for CO. A Principal Component Analysis (PCA) can be employed as a method of extraction of the principal components that could influence CO concentrations and it is applied to a data set of the case study.

PCA takes advantage when a large amount of data is generated in monitoring studies. Through variable reduction and visual display, PCA allows to observe the sources of variation in data set. The principal components are extracted so that the first principal component (PC1) accounts for the largest amount of the total variation in the data, PC2 accounts for the maximum amount of the remaining total variation not already accounted for PC1, etc. In general:

$$PC_i = I_{1i}X_1 + I_{2i}X_2 + \cdots + I_{ni}X_n \quad , \tag{9}$$

where PC_i is *i*-th principal component and I_{ji} is the loading of the observed variable X_j.

The projection of the points from the original space on PCs is called the scores while the score plots depict the linear projection of objects representing the main part of the total variance of the data. Correlation and importance of variables must be decided from plots of the PC loadings. The size of the loadings in relation to the considered principal component is a measure of the importance of a variable for the PC model ([38-40]).

III. Case Study

In Mexico there is not enough information about air pollution and most of the studies about spatial and temporal levels of criteria air pollutants have been focused to Mexico City whose air quality monitoring network began operating in 1966. However, other important urban zones like the Metropolitan Areas Monterrey and Guadalajara started measuring of air pollution until 1992, thus the lack of air quality information is even greater.

This study is focused on San Nicolas de Garza, one of the twelve municipalities of the Metropolitan Area of Monterrey (MAM), which constitutes the third largest urban area in Mexico. MAM is a high profile center of education, tourism and business with a population of 4,000,000 habitants. This city is located at 25°40'N and 100°18' W at 537 masl and covering an area of 580.5 km^2. This area is characterized by the presence of important education and research centers, business activities and industrial development. Road transportation and area sources (evaporative emissions from solvents, storage tanks, coatings, fuel marketing and other miscellaneous sources) are the dominant sources of O_3 precursors in MAM [41].

The Nuevo León State Government has been committed to

undertaking all necessary steps to protect public health from air pollution, with sensitivity to the impacts of its actions on the community and industrial activities. Although air pollutants and weather conditions have been measured from 90's and some actions have been taken in order to improve air quality, some pollutants may reach unhealthy levels during air pollution episodes. In Mexico, with respect to carbon monoxide, significant advances have been made since the implementations by 2012 of a emissions limit from vehicles (ranged from 3.418 to 4.536 g/km depending on the net weight of the vehicle and fuel type) [42]. In addition, a standard to protect population health against CO was implemented in 1993, which regulates the ambient air levels of this pollutant within a limit of 11 ppm (12.595 $\mu g/m^3$) in an 8-h mobile average once a year as maximum [43]. Nevertheless, a better understanding of the behaviour and trends of this pollutant in MAM is required in order to develop effective strategies focused to ozone abatement in this area. This paper describes the methodology for time series analysis of air quality data and the development of a predictive model for daily mean concentrations of CO, and gives an example of this model application in order to predict CO levels from data obtained at the air quality monitoring network of the Integrated System of Environmental Monitoring (SIMA) of Monterrey, Nuevo Leon, Mexico.

A. Case study area description

San Nicolas de los Garza, Nuevo León, Mexico is located at the northeast of the Metropolitan Area of Monterrey (Figure 1). Climate in this area is classified as semi-arid warm being hot in summer (temperature reaches 35 °C in August), though reasonably pleasant in spring and autumn. The average temperature in winter is 8 °C. Rainfall is scarce, but more prominent during May to September. Humidity in winter can be high, although without showers. Snowfall is a very rare event. The annual average precipitation is 615 mm and this area is commonly influenced by frontal systems coming from the north of the continent. The specific sampling site was located within the facilities of Northeast Station of the SIMA, located in the Laboral Unity District in San Nicolas de los Garza, N.L. at 25° 43' 30 "N and 100° 18' 48" W at 500 m above sea level, within an area with high density of population (Figure 2).

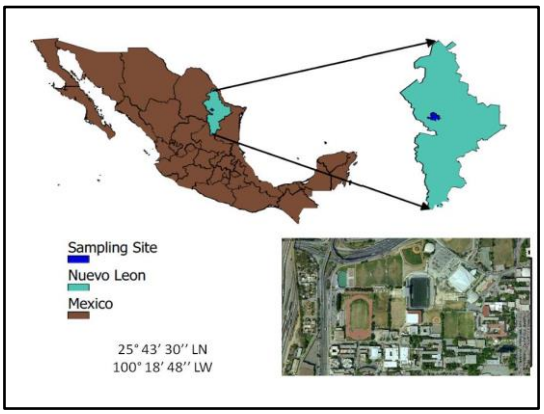

Fig. 1: Case study location

B. Air pollution and meteorological parameters monitoring

The air quality monitoring network of MAM is operated by the Integrated System of Environmental Monitoring (SIMA) of the Mexican Environmental Protection Agency (APMARN). This network has 8 fixed monitoring stations and a Sodar Doppler System for meteorological conditions measuring. Each monitoring station generates hourly information of the ambient air concentrations of criteria air pollutants and meteorological parameters [44]. Table 1 lists the criteria air pollutants (O_3, NO, NO_2, NO_x, CO, PM10, and SO_2) and meteorological parameters (wind direction, wind speed, relative humidity, temperature, solar radiation and barometric pressure) usually measured in the air quality monitoring stations and measurement techniques. The data set used in this paper was limited to hourly CO ambient air concentrations during 2012, obtained from the Northeast Station of the SIMA whose location is indicated in Figure 2.

Table 1: Criteria air pollutants and meteorological parameters usually measured in the air quality monitoring network of MAM

Variable	Measurement Technique	Units
Carbon monoxide (CO)	IR non dispersive attenuation GFG	ppm
Ozone (O_3)	UV spectrophotometer	ppb
Nitrogen dioxide (NO_2)	chemical luminescence	ppb
Sulfur dioxide (SO2)	UV pulsed fluorescence	ppb
Particulate matter with aerodynamic radius equal or lower than 10 µm (PM10)	Beta ray attenuation	$\mu g/m^3$
Wind speed	Conventional anemometer	km/h
Wind direction	Conventional vane	Azimuth grades
Ambient temperature	Solid state thermostat	Celsius grades
Solar radiation	Pyranometer	kW/m^2
Barometric pressure	Barometric pressure sensor	mm Hg

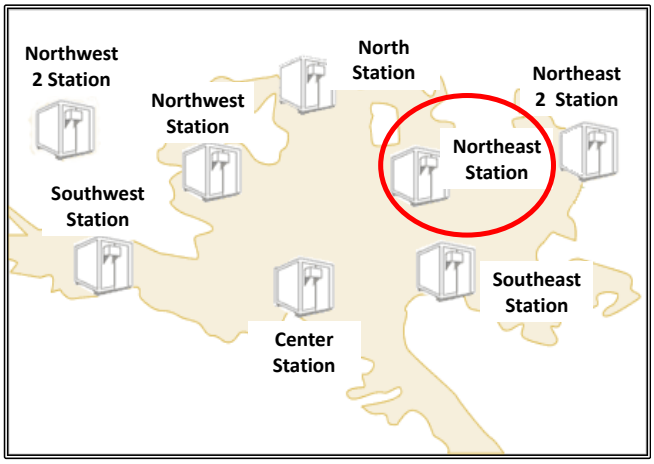

Fig. 2: Specific location of the northeast station within the air quality monitoring network in MAM.

IV. Data analysis and results

A. Calibration phase

The first step, in order to build the model, is to analyse the dataset to be used in the calibration phase. The choice was to consider the CO concentrations, during all the year 2012.

The calibration dataset is made of 8784 hourly CO concentrations, measured in ppm, and the summary statistics are resumed in Table 2. As it can be noticed from skewness and kurtosis values, the distribution is not normal. In addition, the high value of standard deviation with respect to the mean, together with the maximum and minimum values, exploits a very spread distribution.

Table 2: Summary of statistics of the calibration data set, 8784 data, in ppm.

Mean [ppm]	Std.dev [ppm]	Median [ppm]	Min [ppm]	Max [ppm]	skew	kurt
0.66	0.67	0.47	0.08	10.01	5.22	40.96

Looking at the time slope of the data, these CO concentrations show a daily periodic pattern, together with an average decrease in spring and summer. The daily periodic pattern can be explained from distinct peaks which correspond to morning rush hours. This is consistent with the assumption that on-road vehicles dominate CO emissions.

The seasonal pattern of tropospheric CO, with its maximum in winter and its minimum in summer and spring, has been reported before by other authors ([45-49]). The boundary layer usually becomes deeper in late spring and summer because of greater solar insolation and stronger turbulent eddies. This condition promotes released pollutants dilution at the surface and results in lower ambient concentrations [45]. Therefore, during summer, photochemical activity is increased and OH concentrations are higher. In the presence of sunlight and sufficient amount of NO_x (urban atmospheres), photo-oxidation cycle of CO begins with its reaction with OH leading to the tropospheric ozone formation. The lifetime of CO is sufficiently long (from some days over continents in summer to over a year at high latitudes in winter) [46]. Thus, higher OH concentrations and hence a decrease in the lifetime of CO during late spring and summer result in a decrease in tropospheric CO levels. On the other hand, during winter, a longer lifetime of CO result in an accumulation of this pollutant toward late spring until loss by OH surpasses inputs of CO (emissions and photochemical production) [47]. In addition, during winter months, thermal inversions and a decrease in the boundary layer depth contribute to higher CO levels.

By plotting the CO concentration duration curve (Fig. 3), i.e. the plot of the observed concentration sorted in descending order of magnitude rather than chronologically, it is easy to notice that about the 88% of the measurements are below 1 ppm. In the remaining percentage there are strong deviations from the average concentrations that will affect the performances of the model in the validation phase.

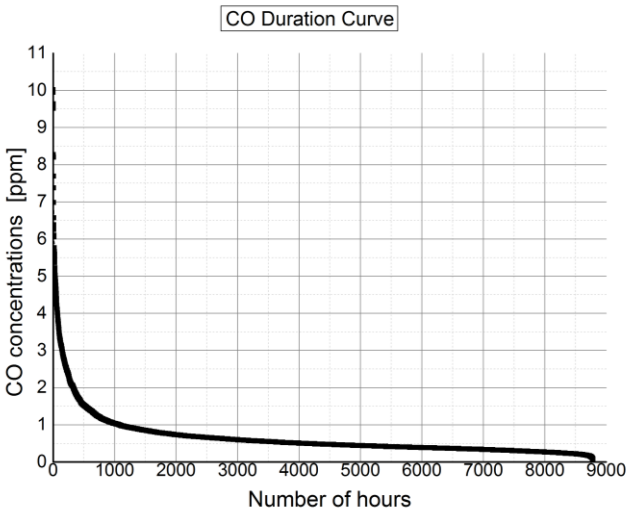

Fig. 3: CO concentrations sorted by descending order of magnitude. The *x* axis reports the number of hours in which the corresponding concentration is exceeded.

In order to check the presence of autocorrelation in the data, the Ljung-Box (LB) and Box-Pierce (BP) tests have been performed. Results are reported in Table 3. The small *p*-value in both tests, i.e. the very small probability to observe the sample if the null hypothesis is true indicates that the hypothesis of absence of autocorrelation in the data can be rejected.

Table 3: Ljung-Box and Box-Pierce tests performed on the 8784 measurements of the calibration dataset.

Type of test	χ^2	*h*	*p*-value
Ljung-Box	33633.9	50	< 2.2e-16
Box-Pierce	33572.66	50	< 2.2e-16

The autocorrelation analysis on the entire calibration dataset, made by means of correlogram, highlights the presence of a 24 hours periodicity, as shown in Figure 4. The autocorrelation value corresponding to a lag of 24 hours is 0.371 .

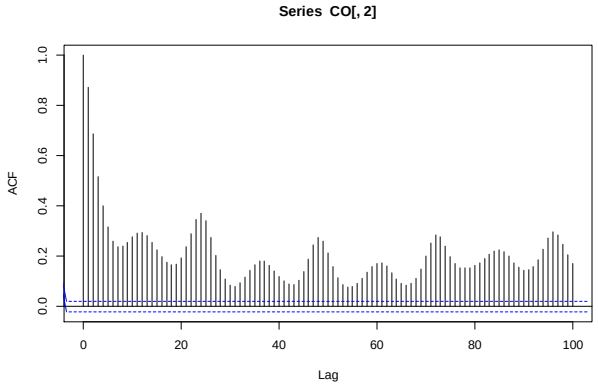

Fig. 4: Autocorrelation plot (correlogram) as a function of the lag (periodicity).

Once the lag has been detected, the model has been built according to procedure described in Section II and in [28]. The

results of the model are plotted in Figure 5, together with the observed CO concentrations. In Table 4, the model parameters are reported. It can be highlighted that the trend line is almost constant and that the seasonal coefficients increase in rush hours, since the corresponding data are affected by vehicles emissions.

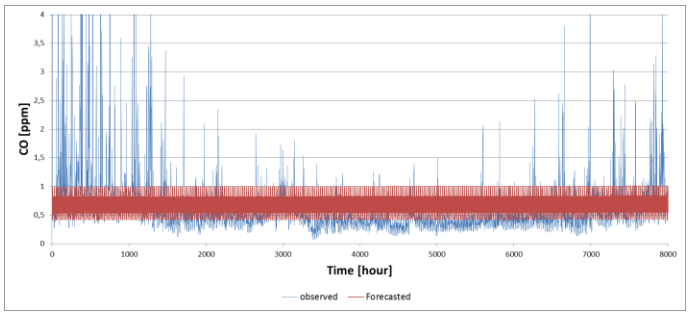

Fig. 5: Observed and predicted CO concentrations, during 2012 (i.e. calibration dataset).

Table 4: Model parameters estimated on the 2012 CO concentration data. b_0 and b_1 are respectively the intercept and the slope of the trend line, while $\bar{S}_i$ is the seasonal coefficient in the time range from *i*-1 to *i* hour.

Time Series Model parameters			
b_0	0,64383730	b_1	0,00000147
$\bar{S}_1$	0,805094	$\bar{S}_{13}$	0,886475
$\bar{S}_2$	0,723286	$\bar{S}_{14}$	0,847639
$\bar{S}_3$	0,680476	$\bar{S}_{15}$	0,839873
$\bar{S}_4$	0,644032	$\bar{S}_{16}$	0,835991
$\bar{S}_5$	0,657638	$\bar{S}_{17}$	0,8627
$\bar{S}_6$	0,845082	$\bar{S}_{18}$	0,9359
$\bar{S}_7$	1,23911	$\bar{S}_{19}$	1,075612
$\bar{S}_8$	1,542119	$\bar{S}_{20}$	1,24604
$\bar{S}_9$	1,469525	$\bar{S}_{21}$	1,274936
$\bar{S}_{10}$	1,237873	$\bar{S}_{22}$	1,182683
$\bar{S}_{11}$	1,038506	$\bar{S}_{23}$	1,08388
$\bar{S}_{12}$	0,939687	$\bar{S}_{24}$	0,953364

It is interesting to notice that the general trend of the time series is achieved, even if the local strong variations are not predicted by the model. These local strong oscillations may be due to daily variations related to meteorological conditions (transport) and emission local sources strength. The model calibration results are described by the error, evaluated according to formula (2). In Table 5, the error statistics are resumed: the mean is close to zero but the maximum value is 9.57 ppm.

Performing the *t*-test in the "*R*" software framework, it has been obtained that the mean error is not statistically different from zero. In particular, the *t*-statistic calculated on the errors in the calibration phase, is 1.778907. The corresponding probability of observing the sample, if the null hypothesis of zero mean is true, is 0.03764476. This value is generally considered too high to reject the null hypothesis.

Thus, the first consideration that can be drawn is that this model is not able to locally predict the exact behaviour of the CO concentration, but it can give interesting results on a long term analysis basis and it can give reliable predictions in periods in which there are not strong variations with respect to the general trend. For instance, the comparison between observed values and model predictions in the range between 7000 and 7500 hours (Figure 6) is encouraging, even if the single peaks are not reconstructed by the model. On the contrary, during the summer time, the model clearly overestimates the observed values.

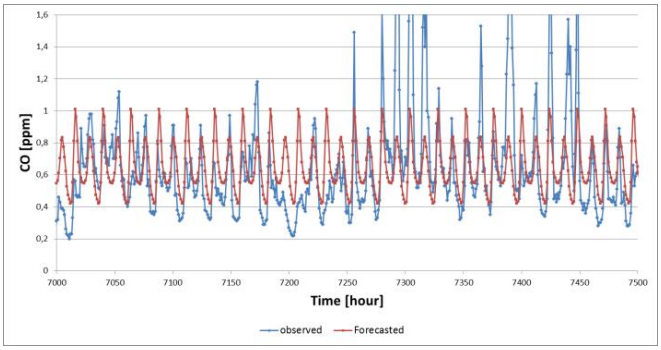

Fig. 6: Observed and predicted CO concentrations, during 2012: zoom on the time range from 7000 to 7500 hours.

Table 5: Summary of statistics of the error distribution, evaluated on the calibration dataset, in ppm.

Mean [ppm]	Std.dev [ppm]	Median [ppm]	Min [ppm]	Max [ppm]
0.01	0.65	-0.15	-0.79	9.57

B. Validation phase

In order to validate the model and to check its performances, a comparison between model predictions and observed CO concentrations has been made on two sample datasets in 2013.

The first validation has been made on January 2013 data (Figure 7): the model hardly predicts the peaks, while the trend seems to be confirmed.

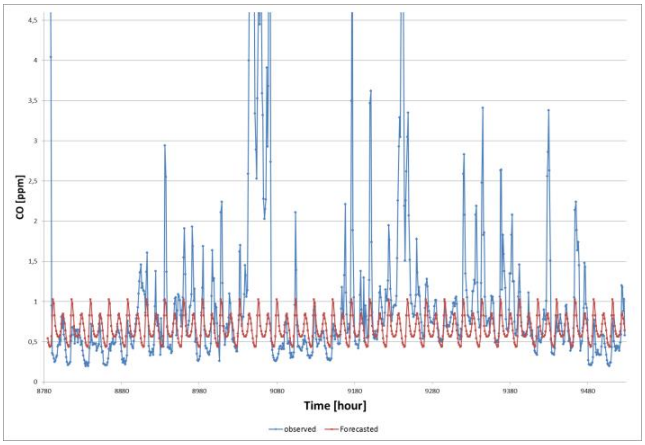

Fig. 7: Observed and predicted CO concentrations, during January 2013 (i.e. first validation dataset).

This is verified also analysing the error distribution (difference between observed and forecasted values, formula 2), whose statistics are reported in Table 6. The general assumption of normal distribution for the errors (residuals) of the model is not achieved in this validation period. The histogram (Figure 8) and the Q-Q plot (Figure 9), in fact, are strongly deviating from the normal pattern, being the first very skewed and the second very far from the bisector.

Table 6: Summary of statistics of the error distribution, evaluated on the first validation dataset (January 2013).

Mean [ppm]	Std.dev [ppm]	Median [ppm]	Min [ppm]	Max [ppm]
0.34	1.09	0.03	-0.75	8.00

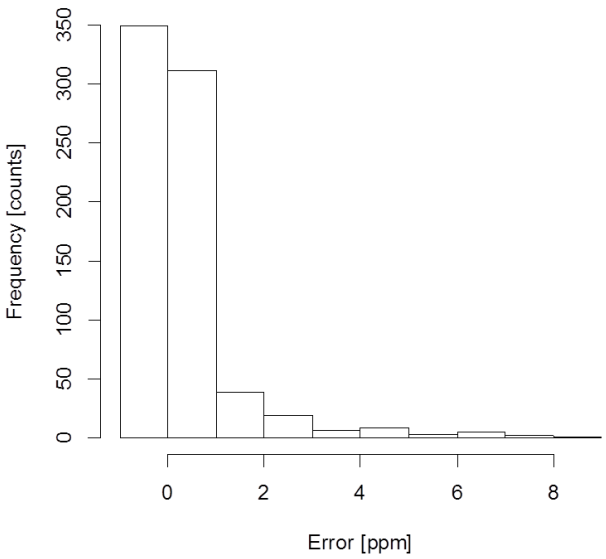

Fig. 8: Frequency histogram of the errors calculated on the first validation dataset, performed on the 744 January data.

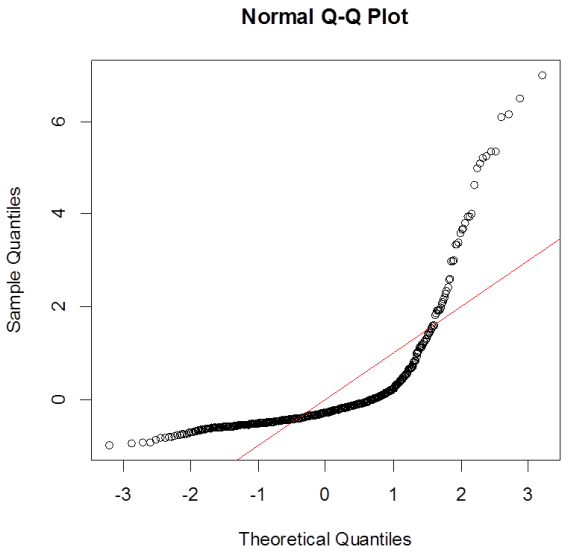

Fig. 9: Normal probability plot that describe error behaviour of the model applied to the 744 January data.

Considering a second validation period, May 2013, when comparing results of the model with observed values, the improvement of the agreement is evident (Figure 10) and confirmed by error distribution statistics (Table 7). Also the histogram of the errors, shown in Figure 11, has a regular shape, that suggests an almost normal distribution of the error. The same can be deduced by the Q-Q plot (Figure 12), in which the sample quantiles approximate the theoretical normal ones, gathering along the bisector, except for the right tail.

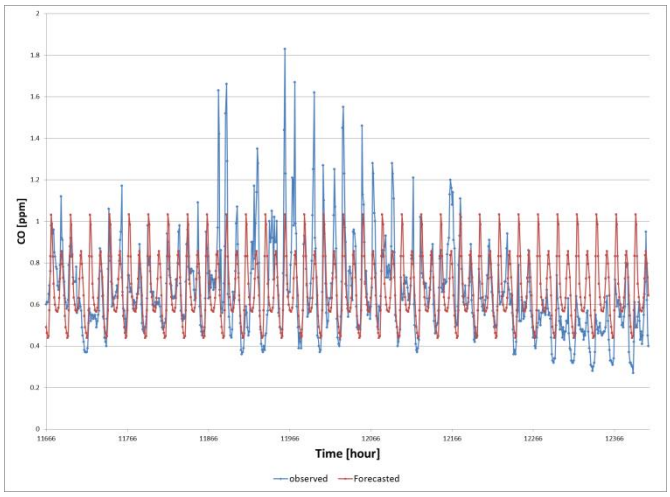

Fig. 10: Observed and predicted CO concentrations, during May 2013 (i.e. second validation dataset).

Table 7: Summary of statistics of the error distribution, evaluated on the second validation dataset (May 2013).

Mean [ppm]	Std.dev [ppm]	Median [ppm]	Min [ppm]	Max [ppm]
-0.01	0.20	-0.02	-0.58	0.84

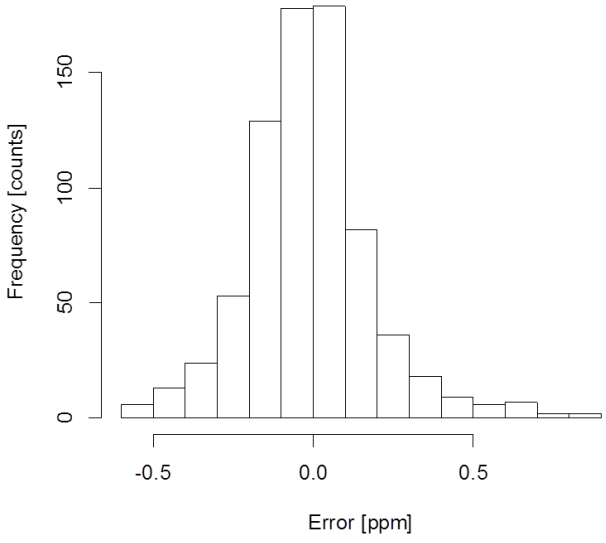

Fig. 11: Frequency histogram of the errors calculated on the second validation dataset, performed on the 744 May data.

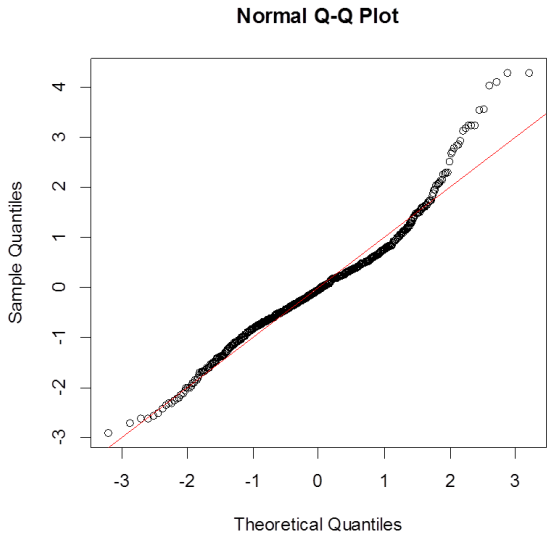

Fig. 12: Normal probability plot that describe error behaviour of the model applied to the 744 May data.

The Mean Percentage Error (MPE) and the Coefficient of Variation of the Error (CVE), presented in Section II, are reported in Table 8, calculated in both the validation datasets. It can be noticed that the MPE seems to worsen in May, while CVE decreases. A so strong overestimation, highlighted by the high negative MPE evaluated in May dataset, can be explained considering that in the last part of the month, the measured values have a substantial reduction with respect to the trend. In fact, if the MPE is computed on 500 data, i.e. excluding the part in which the model overestimates the data (see Figure 10), the results is -0.2 .

Table 8: MPE and CVE (error metrics) values, calculated in the two different validation periods.

Validation dataset	MPE	CVE
January	-4.4	1.136
May	-7.5	0.298

Considering the results of the two different validations, let us underline that, while the mean has a drastic change, the median of the error distribution is slightly different (from 0.03 to -0.02 ppm). This is due to the fact that the median is much less sensitive to distribution outliers than the mean, i.e. in our case, it is not strongly affected by local CO concentration peaks.

Another consideration is that one should expect that the model works better on validation periods closer to calibration dataset. In this case, the model shows better performances on the May 2013 validation period, even if the calibration is done on 2012 data. This is probably due to the fact that in this period there is a lower variability in the data and the slope is closer to the model trend and periodicity, evaluated on 2012 data.

C. PCA Results

PCA was applied by using data for one year period (2012) in order to obtain the relation among CO and other measured parameters (meteorological conditions: solar radiation, wind speed, wind direction, temperature, barometric pressure and relative humidity; and other air criteria pollutants: O_3, NO, NO_2, NO_x, PM_{10}, $PM_{2.5}$ and SO_2). PCA helps to decrease the number of components explaining CO formation. PCs with eigenvalues near to 1 are usually considered as being of statistical significance. In Table 9, it can be observed that the first three PCs accounted 58.792% of the total variance.

Table 9: Explanation of the total variance for the data set of the case study.

Total variance explained			
Component	Initial eigenvalues		
	Total	% of Variance	% Cumulative
PC1	4.525	32.322	32.322
PC2	2.127	15.190	47.512
PC3	1.57	11.280	58.792

PCs obtained from PCA analysis of 13 different input variables were determined by considering coefficients presented in Table 10. Variables affecting CO formation were decreased to three principal groups after PCA applications as it can be observed in Figure 13. PCs with the highest eigenvalues can be used in a multiple regression analysis so formation of CO could be explained. They are useful in exploring the relations among the independent variables particularly if it is not obvious which of the variables should be good predictors. In this case good predictor variables could be P, NO_2, NOx, PM_{10}. $PM_{2.5}$, T, and SR. Therefore, usage of PCA provides process facilities for the models working with numerous variables ([50-52]).

Table 10: Factor loadings for the three principal components. Only eigenvalues greater than 0.5 are shown.

Variables	PC1	PC2	PC3
WSR (Wind speed)	-0.626	-	-
WDR (Wind direction)	-	-	-
T (temperature)	-0.519	0.695	-
RH (relative humidity)	-	-0.573	-
P (barometric pressure)	0.542	-	-
CO (carbon monoxide)	0.910	-	-
NO (nitrogen monoxide)	-	-	-
O_3 (ozone)	-	-	-
NO_2 (nitrogen dioxide)	0.774	-	0.673
NO_x (nitrogen oxides)	0.542	-	-
PM_{10} ((particulate matter with aerodynamic radius equal or lower than 10 μm)	0.729	-	-
$PM_{2.5}$ (particulate matter with aerodynamic radius equal or lower than 2.5 μm)	0.648	-	-
SR (solar radiation)	-0.569	0.616	-

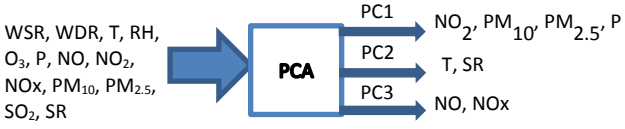

Fig. 13: PCs obtained from PCA analysis and variables influencing CO concentrations.

Figure 14 shows the biplot and factor loadings for two of the three main components (PC1 and PC2). In addition, Pearson correlation matrix was constructed from the data set (Table 11) where it can be observed that CO showed a significant positive correlation with NO_2, PM_{10} and $PM_{2.5}$ (Pearson correlation coefficients of 0.726, 0.670 and 0.617, respectively), indicating that these pollutants could have a common origin, probably from vehicular emissions. Whereas, a negative moderate correlation was found between CO and wind speed (-0.568) indicating that at least partially, dispersion phenomena could decrease CO concentrations in the studied site.

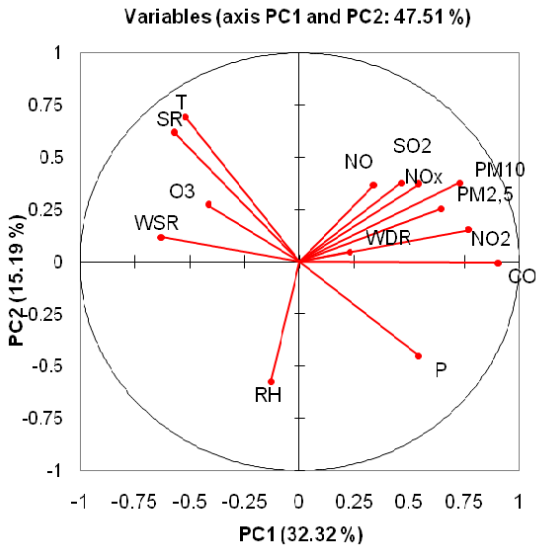

Fig. 14: Biplot and factor loadings for PC1 and PC2.

Table 11: Pearson correlation matrix for the measured variables and CO concentrations.

Variables	CO
WSR	**-0.568**
WDR	0.146
T	-0.429
RH	-0.058
O_3	-0.395
P	0.455
CO	1
NO	0.213
NO_2	**0.726**
NOx	0.407
PM_{10}	**0.670**
$PM_{2.5}$	**0.617**
SO_2	0.397
SR	-0.438

V. Conclusions

In this paper the authors deal with the problem of modelling the time series of Carbon Monoxide (CO) concentrations in the urban site of San Nicolas de los Garza, Nuevo Leon, Mexico. A mixed Time Series Analysis (TSA) model, i.e. a model that considers a multiplicative relation between trend and seasonality of the data, and an additive correction related to the calibration error, has been adopted. This model has been calibrated on the 2012 CO concentration data, obtaining a 24 hours periodicity and an almost constant trend. The error in the calibration has been evaluated as the difference between observed and forecasted values, and its mean has been added to the product between trend and seasonality, in order to obtain the final model. The validation of the resulting model has been performed on two different periods (January and May) of 2013 CO concentration dataset, giving different results. In particular, the second validation dataset shows better results in terms of error statistics and normality of the distribution. This is probably due to the fact that in this period there is a lower variability in the data and the slope is closer to the model trend and periodicity, evaluated in the calibration phase. Even though the graphical comparison and the error means in the two validation datasets are strongly different, the median of the error distribution is similar in both periods. The median, in fact, is a better measure of central tendency with respect to the mean, in case of random peaks presence in the dataset.

In addition, a PCA was applied by using hourly measured data (meteorological parameters and air criteria pollutants concentrations) for one year period in order to reduce the number of input variables to be used in future multiple regressions modelling in order to predict CO concentrations. Resulting principal components (PCs) contain the following variables: barometric pressure (P), nitrogen dioxide (NO_2), nitrogen oxides (NOx), particulate matter (PM_{10} and $PM_{2.5}$), Temperature (T), and solar radiation (SR). These PCs could become ideal to use as predictors in a multiple regression equation since they optimize spatial patterns and remove possible complications caused by multicollinearity.

Finally, it can be affirmed that the TSA model presented in this paper is able to predict the general slope of the data, while local variations and random peaks are hard to be predicted. Further studies on multiple periodicity or different regression methods represent the next steps of this analysis, and will be postponed to future works.

Acknowledgment

The authors are grateful to the local Government of San Nicolas de los Garza, Nuevo Leon, especially to the Integrated System of Environmental Monitoring (SIMA), for having made available the air pollutants levels data measured in MAM used in this paper.

REFERENCES

[1] Sousa, S.I.V., Martins, F.G., Pereira, M.C., and Alvim-Ferraz, M.C.M 2006. Prediction of ozone concentrations in Oporto City with statistical approaches. Chemosphere 64, 1141-1149.

[2] Van Eijkeren, J.C., Freijer, J.I., and Van Bree, L. 2002. A model for the effect on health of repeated exposure to ozone. Environmental Modelling and Software 17, 553-562 .

[3] Xu, J., and Zhu, Y. 1994. Some characteristics of ozone concentrations and their relations with meteorological factors in Shangai. Atmospheric Environment 20, 3387-3392.

[4] Lee, D.S., Holland, M.R., and Falla, W. 1996. The potential impact of ozone on materials in the U.K. Atmospheric Environment 30 (7), 1053-1065.

[5] Cass, G.R., Nazarof, W.W., Tiller, C., and Whitmore, P.M. 1991. Protection of works of art from damage due to the atmospheric ozone. Atmospheric Environment 25A, 441-451.

[6] Wang, S.W. and Georgopoulos, P.G. 2001. Observational and mechanistic studies of tropospheric studies of ozone, precursor relations: photochemical models performance evaluation with case study. Technical Report ORC-TR99-03.

[7] Cerón-Bretón, J.G., Cerón-Bretón, R.M., Guerra-Santos, J.J., Córdova-Quiroz, A.V., Vargas-Cáliz, C., Aguilar-Bencomo, L.G., Rodriguez-Heredia, K., Bedolla-Zavala, E., and Pérez-Alonso, J. 2010 a. Effects of simulated tropospheric ozone on soluble proteins and photosynthetic pigments levels of four woody species typical from the Mexican Humid Tropic. WSEAS Transactions on Environment and Development 6 (5), 335-344.

[8] Cerón-Bretón, J.G., Cerón-Bretón, R.M., Rangel-Marrón, M., Vargas-Cáliz, C., Aguilar-Bencomo, L.G., and Muriel-García, M. 2010 b. Effects of simulated tropospheric ozone on foliar nutrients levels (Ca2+, Mn2+, Mg2+, and K+) of three woody species of high commercial value typical from Campeche, Mexico. WSEAS Transactions on Environment and Development 6 (11), 731-743.

[9] Aris, R.M., Christian, D., Hearne, P.Q., Kerr, K., Finkbeiner, W.E., and Balmes, J.R. 1993. Ozone-induced airway inflammation in human subjects as determined by airway lavage and biopsy. Am. Rev. Respir. Dis. 148, 1363-1372.

[10] Coleridge, J.C., Coleridge, H.M., Schelegle, E.S., and Green, J.F. 1993. Acute inhalation of ozone stimulates bronchial C-fibers and rapidly adapting receptors in dogs. J. Appl. Physiol. 74, 2345-2352.

[11] Cashel, P., Newhouse, B.S., and Leventin, E. 2004. Correlation of environmental factors with asthma and rhinitis symptons in Tulsa, OK. Ann. Allergy, Asthma & Immun. 92, 356-366.

[12] Hampson, N.B. 1998. Emergency Department visits for carbon monoxide poisoning. Journal of Emergency Medicine 16, 695-698.

[13] U.S. EPA. Environmental Protection Agency Office of Mobile Sources. Motor vehicles and the 1990 Clean Air Act, August, 1994.

[14] Crutzen, J. 1974. Photochemical reactions initiated by and influencing ozone in unpolluted tropospheric air. Tellus, Vol. 26, 47-56.

[15] Finlayson-Pitts, B.J., and Pitts, J.N. Jr. 1999. Chemistry of the upper and lower atmosphere: Theory, Experiments and Applications. Academic Press, San Diego, CA, USA, 90-96.

[16] Guarnaccia C., Advanced Tools for Traffic Noise Modelling and Prediction, WSEAS Transactions on Systems, Issue 2, Vol.12, 2013, pp. 121-130.

[17] Quartieri J., Mastorakis N. E., Iannone G., Guarnaccia C., D'Ambrosio S., Troisi A., Lenza T.L.L, A Review of Traffic Noise Predictive Models, Proceedings of the 5th WSEAS International Conference on "Applied and Theoretical Mechanics" (MECHANICS'09), Puerto de la Cruz, Tenerife, Spain, 14-16 December 2009, pp. 72-80.

[18] Quartieri J., Troisi A., Guarnaccia C., Lenza TLL, D'Agostino P., D'Ambrosio S., Iannone G., An Acoustical Study of High Speed Train Transits, WSEAS Transactions on Systems, Issue 4, Vol.8, pp. 481-490 (2009).

[19] Quartieri J., Troisi A., Guarnaccia C., Lenza TLL, D'Agostino P., D'Ambrosio S., Iannone G., Application of a Predictive Acoustical Software for Modelling Low Speed Train Noise in an Urban Environment, WSEAS Transactions on Systems, Issue 6, Vol.8, pp. 673-682 (2009).

[20] Guarnaccia C., Lenza T.LL., Mastorakis N.E., Quartieri J., A Comparison between Traffic Noise Experimental Data and Predictive Models Results, International Journal of Mechanics, Issue 4, Vol. 5, pp. 379-386 (2011), ISSN: 1998-4448.

[21] Guarnaccia C., Mastorakis N.E., Quartieri J., Wind Turbine Noise: Theoretical and Experimental Study, International Journal of Mechanics, Issue 3, Vol.5, pp. 129-137 (2011).

[22] Guarnaccia C., Analysis of Traffic Noise in a Road Intersection Configuration, WSEAS Transactions on Systems, Issue 8, Volume 9, (2010), pp.865-874, ISSN: 1109-2777.

[23] Iannone G., Guarnaccia C., Quartieri J., Speed Distribution Influence in Road Traffic Noise Prediction, Environmental Engineering And Management Journal, Vol. 12, Issue 3, 2013, pp. 493-501.

[24] Rodrigues, E.R., Achcar, J.A., and Jara-Ettinger, J. A Gibbs sampling algorithm to estimate the occurrence of ozone exceedances in Mexico City. In: Air Quality: Models and Applications, Popovic D (ed.), In Tech Open Access Publishers, 131-150, 2011.

[25] Achcar, J.A., Fernandez-Bremauntz, A.A., Rodrigues, E.R., and Tzintzun, G., Estimating the number of ozone peaks in Mexico City using a non homogeneous Poisson model, Environmetrics, 19, 469-485, 2008.

[26] Box, G. E. P., and Jenkins, G., Time Series Analysis: Forecasting and Control, Holden-Day, 1976.

[27] Chatfield, C., The Analysis of Time Series: an Introduction, Chapman & Hall, New York, 1975.

[28] Guarnaccia C., Quartieri J., Mastorakis N. E. and Tepedino C., Acoustic Noise Levels Predictive Model Based on Time Series Analysis, in "Latest Trends in Circuits, Systems, Signal Processing and Automatic Control", proceedings of the 2nd Int. Conf. on Acoustics, Speech and Audio Processing (ASAP '14), Salerno, Italy, June 3-5, 2014 , ISSN: 1790-5117, ISBN: 978-960-474-374-2, pp. 140-147.

[29] Guarnaccia C., Quartieri J., Rodrigues E. R. and Tepedino C., Time Series Model Application to Multiple Seasonality Acoustical Noise Levels Data Set, in "Latest Trends in Circuits, Systems, Signal Processing and Automatic Control", proceedings of the 2nd Int. Conf. on Acoustics, Speech and Audio Processing (ASAP '14), Salerno, Italy, June 3-5, 2014 , ISSN: 1790-5117, ISBN: 978-960-474-374-2, pp. 171-180.

[30] Pope C. A., Dockery D. W., Spengler J. D., and Raizenne M. E., Respiratory Health and PM10 Pollution: A Daily Time Series Analysis, American Review of Respiratory Disease, Vol. 144, No. 3_pt_1 (1991), pp. 668-674.

[31] Dominici F., McDermott A., Zeger S. L., and SametJ. M., On the Use of Generalized Additive Models in Time-Series Studies of Air Pollution and Health, American Journal of Epidemiology, 156 (3), pp 193-203, 2002.

[32] Di Matteo T., Aste T., Dacorogna M.M., Scaling behaviors in differently developed markets, Physica A: Statistical Mechanics and its Applications, Vol. 324, Issues 1–2, 2003, pp. 183-188.

[33] Milanato D., Demand Planning. Processi, metodologie e modelli matematici per la gestione della domanda commerciale, Springer, Milano, 2008, in Italian.

[34] Chase R. B., Aquilano N. J., Operations Management for Competitive Advantage, Irwin Professional Pub, 10th edition, 2004.

[35] Box, G. E. P., Pierce, D. A., "Distribution of Residual Autocorrelations in Autoregressive-Integrated Moving Average Time Series Models", *Journal of the American Statistical Association*, 65: 1509–1526, (1970).

[36] Ljung G. M., Box, G. E. P., "On a measure of lack of fit in time series models", *Biometrika*, 65, 297-303, (1978).

[37] Chambers, John, William Cleveland, Beat Kleiner and Paul Tukey, *Graphical Methods for Data Analysis*, Wadsworth, 1983.

[38] Lam K.C., Tao R., Lam M.C.K., A material supplier selection model for property developers using Fuzzy Principal Component Analysis, Auto. In Const., Vol. 19 (2010), pp. 608-618.

[39] Lu H.C., Hsieh J.C., Chang T.S., Prediction of daily maximum ozone concentrations from meteorological conditions using a two stage neural network, Atmospheric Research, Vol. 81 (2006), pp. 124-139.

[40] Hsieha K.L., Yang I.C., Incorporating PCA and Fuzzy-ART techniques into achieve organism classification based on codon usage consideration, Comput. Biol. Med., Vol. 38 (2008), pp. 886-893.

[41] SEMARNAT-INE. 2005. Emissions Inventory for the Metropolitan Area of Monterrey.

[42] SEMARNAT. Mexican Environmental Protection Agency. 2012. NOM-076-SEMARNAT-2012: Mexican standard to regulate maximum permissible levels of hydrocarbons, carbon monoxide and nitrogen oxides in vehicle exhaust.

[43] SSA. Mexican Public Health Agency. 1993. NOM-021-SSA1-1993. Mexican standard to regulate air quality for carbon monoxide ambient air concentrations.

[44] SIMA. 2014. Monitoring Program of Nuevo Leon State. http://www.nl.gob.mx/?P=med_amb_mej_amb_sima_municipal
[45] Chen L.W.A., Doddridge B.G., Dickerson R.R., Chow J.C., Mueller P.K., Quinn J., Butter W.A., Seasonal variations in elemental carbon aerosol, carbon monoxide and sulfur dioxide: implications for sources, Geophysical Research Letter, Vol. 28, No. 3 (2001), pp. 1711-1714.
[46] Holloway T., Ley II H.L., Kasibhatla P., Global distribution of Carbon monoxide, Journal of Geophysical Research: Atmospheres, Vol. 105 (2000), pp. 12123-12147.
[47] Koike M., Jones N.B., Palmer P.I., Matsui H., Zhao Y., Kondo Y., Matsumi Y., Tanimoto H., Seasonal variation of carbon monoxide in northern Japan: Fourier transform IR measurements and source-labeled model calculations, Journal of Geophysical Research, Vol. 111 (2006), pp. 1-15.
[48] Novelli P.C., Masarie K.A., Lang P.M., Distributions and changes of carbon monoxide in the lower troposphere, Journal of Geophysical Research: Atmospheres, Vol. 103 (1998), pp. 19015-19033.
[49] Rinsland C.P., Mahieu E., Zander R., Demoulin P., Forrer J., Buchmann B., Free tropospheric CO, C2H6 and HCN above central Europe: Recent measurements from the Jungfraujoch station including the detection of elevated columns during 1998, Journal of Geophysical Research: Atmospheres, Vol. 105 (2000), pp. 24235-24249.
[50] Ozbay B., Keskin G.A., Dogruparmak S.C., Ayberk S., Multivariate methods for ground-level ozone modelling, Atmospheric Research, Vol. 102 (2011), pp. 57-65.
[51] Abdul-Wahab S.A., Bakheitb C.S., AL-Alawi S.M., Principal component and multiple regression analysis in modelling of ground-level ozone and factors affecting its concentrations, Environ. Model. & Soft., Vol. 20 (2005), pp. 263-271.
[52] Sousa S.I.V., Martins F.G., Alvim-Ferraz M.C.M., Pereira M.C., Multiple linear regression and artificial neural networks based on principal components to predict ozone concentrations, Environ.Model & Soft., Vol. 22 (2007), pp. 97-103.
[53] Quartieri J., Troisi A., Guarnaccia C., D'Agostino P., D'Ambrosio S., Iannone G., Development of an Environmental Quality Index Related to Polluting Agents, Proceedings of the WSEAS International Conference on "Environment, Ecosystem and Development" (EED'09), Puerto de la Cruz, Tenerife (Spain), 14-16 December 2009, pp. 153-161.
[54] Quartieri J., Iannone G., Guarnaccia C., On the Improvement of Statistical Traffic Noise Prediction Tools, Proceedings of the 11th WSEAS International Conference on "Acoustics & Music: Theory & Applications" (AMTA '10), Iasi, Romania, 13-15 June 2010, pp. 201-207.
[55] Quartieri J., Mastorakis N. E., Guarnaccia C., Troisi A., D'Ambrosio S., Iannone G., Traffic Noise Impact in Road Intersections, International Journal of Energy and Environment, Issue 1, Volume 4 (2010), pp. 1-8.
[56] Iannone G., Guarnaccia C., Quartieri J., Noise Fundamental Diagram deduced by Traffic Dynamics, in "Recent Researches in Geography, Geology, Energy, Environment and Biomedicine", Proceedings of the 4th WSEAS Int. Conf. on Engineering Mechanics, Structures, Engineering Geology (EMESEG '11), Corfù Island, Greece, July 14-16, 2011, pp. 501-507.
[57] Quartieri J., Mastorakis N.E., Guarnaccia C., Iannone G., Cellular Automata Application to Traffic Noise Control, Proc. of the 12th Int. Conf. on "Automatic Control, Modelling & Simulation" (ACMOS '10), Catania (Italy), 29-31 May 2010, pp. 299-304.
[58] Guarnaccia C., Acoustical Noise Analysis in Road Intersections: a Case Study, Proceedings of the 11th WSEAS International Conference on "Acoustics & Music: Theory & Applications" (AMTA '10), Iasi, Romania, 13-15 June 2010, pp. 208-215.
[59] Guarnaccia C., New Perspectives in Road Traffic Noise Prediction, in "Latest advances in Acoustics and Music", proceedings of the 13th Int. Conf. on Acoustics & Music: Theory & Applications (AMTA '12), Iasi, Romania, 13-15 June 2012. ISBN: 978-1-61804-096-1, pp. 255-260
[60] Quartieri J., Troisi A., Guarnaccia C., Lenza TLL, D'Agostino P., D'Ambrosio S., Iannone G., Analysis of Noise Emissions by Train in Proximity of a Railway Station, Proceedings of the 10th International Conference on "Acoustics & Music: Theory & Applications" (AMTA '09), Prague (Rep.Ceca), 23-25 March 2009, pp: 100-107.
[61] Quartieri J., Troisi A., Guarnaccia C., Lenza TLL, D'Agostino P., D'Ambrosio S., Iannone G., An Italian High Speed Train Noise Analysis in an Open Country Environment, Proceedings of the 10th International Conference on "Acoustics & Music: Theory & Applications" (AMTA '09), Prague (Rep.Ceca), 23-25 March 2009, pp: 92-99.
[62] Quartieri J., Mastorakis N. E., Guarnaccia C., Troisi A., D'Ambrosio S., Iannone G., Road Intersections Noise Impact on Urban Environment Quality, Proceedings of the 5th WSEAS International Conference on "Applied and Theoretical Mechanics" (MECHANICS '09), Puerto de la Cruz, Tenerife, Spain, 14-16 December 2009, pp. 162-171.
[63] Guarnaccia C., Quartieri J., Barrios J. M., Rodrigues E. R., Modelling Environmental Noise Exceedances Using non-Homogenous Poisson Processes, accepted and in press, Journal of the Acoustical Society of America, Vol. 136, Issue 4 (2014).
[64] Quartieri J., Sirignano L., Guarnaccia C., Equivalence between Linear and Curved Sources in Newtonian Fields: Acoustics Applications, Proc. Of the Int. Conf. on Engineering Mechanics, Structures, Engineering Geology (EMESEG '08), Heraklion, Crete Island, Greece, July 22-24, 2008, pp: 393-395.
[65] Quartieri J., Sirignano L., Guarnaccia C., Infinitesimal Equivalence between Linear and Curved Sources in Newtonian Fields: Application to Acoustics, International Journal of Mechanics, Issue 4, Vol.1, pp. 89-91 (2007), ISSN: 1998-4448.
[66] Guarnaccia C., Mastorakis N. E., Quartieri J., A Mathematical Approach for Wind Turbine Noise Propagation, in Applications of Mathematics and Computer Engineering, American Conference of Applied Mathematics (AMERICAN-MATH '11), Puerto Morelos, Mexico, 29-31 January 2011, pp. 187-194.